

# IMPLEMENTATION OF THE SVD-BASED PRECODING SUB-SYSTEM FOR THE COMPRESSED BEAMFORMING WEIGHTS FEEDBACK IN IEEE 802.11N/AC WLAN

Yang-Cheng Lin, Tsung-Hsien Liu, Chia-Peng Chou, and Yuan-Sun Chu

National Chung Cheng University  
168 University Rd., Min-Shiung, Chia-Yi, Taiwan

## ABSTRACT

The compressed beamforming weights feedback is used in the precoded MIMO-OFDM system, e.g., IEEE 802.11n/ac WLAN, to reduce the amount of feedback information. The precoded sub-system at the receiver of this system needs to perform singular value decomposition (SVD) on the estimated channel matrices at all sub-carriers. The computed angles of the right singular vectors are to be feedback to the transmitter. Also the computed singular values and left singular vectors are to be used for designing the optimal detector. Under the exemplary scenario of four antennas at the access point and two antennas at the station, our designed architectures for the precoding sub-system can provide SVD throughput rates 16.8 and 50.4 M matrices/sec for the uplink and downlink transmissions, respectively.

**Index Terms**— multiple input multiple output (MIMO) system, precoded MIMO system, singular value decomposition

## 1. INTRODUCTION

Precoding is one of the practical and effective approaches for the multiple input multiple output orthogonal frequency division multiplexing (MIMO-OFDM) system to fight against fading channels [1]. The precoded MIMO-OFDM communication system provides better error rate performance than the space-time coded or spatial division multiplexed MIMO-OFDM system [2, Chap. 13]. However, the major disadvantage of the precoded MIMO-OFDM system is that it requires the channel state information (CSI) estimated at the receiver side to be feedback to the transmitter side. To mitigate the time-varying channel effect, the time difference between the transmission of training pilots and the transmission of precoded data has to be small. One solution to achieve this goal is to reduce the amount of CSI information feedback to the transmitter side.

Two different ways to reduce the amount of CSI information have been adopted by the 3GPP LTE [3–6] and IEEE 802.11n/ac WLAN [2]. In the 3GPP LTE, a codebook of precoding matrices are known to both the transmitter and receiver sides. The receiver estimates the CSI based on the pilots sent by the transmitter. The receiver then determines a codeword from the codebook and sends the index of the codeword only to the transmitter side. Once the transmitter receives the codeword index, it finds the corresponding codeword from the codebook and starts the transmission of the precoded data. In the IEEE WLAN, angles representing the precoding matrices are determined by the receiver and then sent to the transmitter side. This approach is referred to as the compressed beamforming weights feedback, because the information bits to represent the precoding matrices are fewer than the information bits to represent

the true value of the precoding matrices. The transmitter constructs precoding matrices based on the received angles and starts the transmission of the precoded data.

There have been several papers dedicated to the algorithms or hardware architectures for the precoding sub-system in the IEEE 802.11n/ac WLAN. With the estimated CSI, the receiver for the WLAN needs to determine the precoding matrices by applying singular value decomposition (SVD) to the channel matrices at all sub-carriers [7–11]. Let  $\mathbf{H}_k$  be the channel matrix at the  $k$ -th sub-carrier. The SVD of  $\mathbf{H}_k$  produces left singular vectors in  $\mathbf{U}_k$ , right singular vectors in  $\mathbf{V}_k$ , and singular values in  $\Sigma_k$ . Givens rotation was used to compute matrices  $\mathbf{V}_k$  and  $\Sigma_k$  [7]. Subspace tracking algorithm was used to compute the matrices  $\mathbf{V}_k$  and  $\Sigma_k$  in [9]. Subspace tracking algorithms were used to compute the matrices  $\mathbf{V}_k$ ,  $\mathbf{U}_k$ , and  $\Sigma_k$  in [8, 10]. From the viewpoint of receiver design, these architectures only compute the non-compressed beamforming weights for the 11n/ac WLAN. They do not compute the compressed beamforming weights, because they do not compute the angles to represent  $\mathbf{V}_k$ . Additionally, the matrices  $\mathbf{U}_k$  and  $\Sigma_k$  are used by the receiver to perform optimal detection. It is therefore suggested that all the matrices  $\mathbf{U}_k$ ,  $\Sigma_k$ , and  $\mathbf{V}_k$  should be computed at once.

Our objective in this paper is to propose architectures for the precoding sub-systems that deliver compressed beamforming weights feedback with high SVD throughput rate. Both uplink and downlink transmission for the exemplary antenna system with four antennas at the access point and two antennas at the station will be considered. At the algorithmic level, we will use Givens rotations and Jacobi algorithm [12, 13] to compute the angles. At the architectural level, we will use triangular systolic array and CORDIC modules to achieve high throughput rate.

## 2. THE PRECODED MIMO-OFDM SYSTEM

Consider the precoded MIMO-OFDM system [2] in Fig. 1 over a time-invariant wireless channel. At the transmitter side, a stream of digitally modulated symbols is passed through a spatial stream parser to produce  $N_s$  streams of symbols. A precoder with  $N_t \times N_s$  precoding matrix  $\mathbf{P}_k$  for the  $k$ -th sub-carrier transforms the  $N_s$  spatial streams of data to produce  $N_t$ ,  $N_t \geq N_s$ , spatial streams of data. The resulting streams of data are then inverse discrete Fourier transformed (IDFT) to produce baseband signals for transmission through the  $N_t$  transmit antennas. Assume that there are  $N_r$ ,  $N_r \geq N_s$ , receive antennas. The received equivalent baseband  $N_r \times 1$  signal at time (OFDM symbol)  $n$  and sub-carrier  $k$  can be expressed as

$$\mathbf{x}_{n,k} = \mathbf{H}_k \mathbf{P}_k \mathbf{s}_{n,k} + \mathbf{z}_{n,k}, \quad (1)$$

where  $N_r \times N_t$   $\mathbf{H}_k$  is the equivalent channel matrix at sub-carrier  $k$ ,  $N_s \times 1$   $\mathbf{s}_{n,k}$  is the transmitted vector at time  $n$  and sub-carrier  $k$ , and  $N_r \times 1$   $\mathbf{z}_{n,k}$  is the additive noise at time  $n$  and sub-carrier  $k$ .

This paper was supported in part by the Ministry of Science and Technology, Taiwan, under Contract MOST 103-2221-E-194-012.

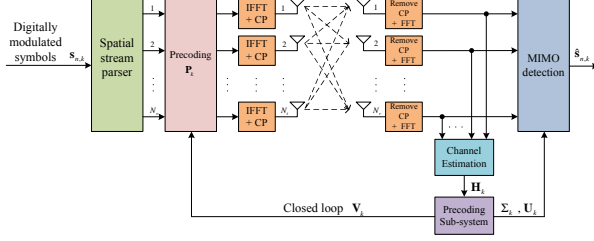


**Fig. 1.** A precoded MIMO-OFDM system with precoding weights feedback.

In practical implementation, the precoding matrices  $\mathbf{P}_k, \forall k$ , have to be determined by the receiver before the precoded data can be transmitted [2]. Initially, the transmitter sends pilots to the receiver such that the estimation of the channel information  $\mathbf{H}_k, \forall k$  can be performed. Immediately later, the receiver computes each precoding matrix  $\mathbf{P}_k$  based on each channel information  $\mathbf{H}_k$ . Values of  $\mathbf{P}_k, \forall k$ , are sent back to the transmitter side so that the transmitter can use these  $\mathbf{P}_k, \forall k$ , to transmit signals in the precoding mode.

Determination of the precoding matrices  $\mathbf{P}_k, \forall k$ , from the channel information  $\mathbf{H}_k, \forall k$ , is the most important work for the receiver of the precoded system. Assume that the SVD of each channel matrix  $\mathbf{H}_k$  is decomposed as

$$\mathbf{H}_k = \mathbf{U}_k \mathbf{\Sigma}_k \mathbf{V}_k^H \quad (2)$$

where  $N_r \times N_r \mathbf{U}_k$  contains orthonormal left singular vectors, diagonal  $\mathbf{\Sigma}_k$  contains singular values in decreasing order, and  $N_t \times N_t \mathbf{V}_k$  contains orthonormal right singular vectors. Each matrix  $\mathbf{P}_k$  is selected to be equal to the sub-matrix of  $\mathbf{V}_k$  that contains the left  $N_s$  columns, i.e., the columns of  $\mathbf{P}_k$  are the right singular vectors of  $\mathbf{H}_k$  that are associated with the largest  $N_s$  singular values. When the precoded signal is transmitted as in (1), the receiver linearly filters the received signal to produce

$$\mathbf{y}_{n,k} \triangleq \mathbf{W}_k^H \mathbf{x}_{n,k} = \text{diag}\{\sigma_1, \dots, \sigma_{N_s}\} \mathbf{s}_{n,k} + \mathbf{W}_k^H \mathbf{z}_{n,k}, \quad (3)$$

where the filter weight  $\mathbf{W}_k$  is equal to the sub-matrix of  $\mathbf{U}_k$  that contains the left  $N_s$  columns. Each entry of  $\mathbf{y}_{n,k}$  is sliced to produce the detected symbol. Note that the above-mentioned design of the precoder and receiver is optimal [1, 14]. Accordingly, the receiver have to perform SVD of each  $\mathbf{H}_k$  to obtain the largest  $N_s$  singular values  $\{\sigma_1, \dots, \sigma_{N_s}\}$ , and, their associated left singular vectors and right singular vectors.

Since the transmit-receive operations for all the sub-carriers are the same, we will ignore the sub-carrier index  $k$  in the following for notational simplicity. The precoded MIMO-OFDM system is simplified to the precoded MIMO system. Additionally, in the IEEE 802.11n/ac WLAN, there are two different ways [2] to feedback the  $\mathbf{V}$  to the transmitter. In non-compressed beamforming weights feedback, the value of  $\mathbf{V}$  is feedback. In compressed beamforming weights feedback, a set of angles representing  $\mathbf{V}$  is feedback. We will concentrate on the compressed beamforming weights feedback, because it sends fewer bits of information back to the transmitter.

In all, we will study the implementation of the precoding sub-system at the receiver side in Fig. 1. The sub-system performs SVD of  $\mathbf{H}$  to produce the largest  $N_s$  singular values  $\{\sigma_1, \dots, \sigma_{N_s}\}$ , the associated right singular vectors to be feedback to the transmitter, and the associated right singular vectors for optimal filtering. Also, the most exemplary case of four and two antennas deployed at the access point (AP) and station, respectively, will be considered.

### 3. PRECODING SUB-SYSTEM FOR THE UPLINK TRANSMISSION

In this section, we will study the precoded sub-system for the uplink transmission with  $N_t = N_s = 2$  and  $N_r = 4$ . We will study the SVD of  $4 \times 2 \mathbf{H}$  to produce  $4 \times 2 \mathbf{U}$ ,  $2 \times 2 \mathbf{\Sigma}$ , and  $2 \times 2 \mathbf{V}$ . The values of  $\mathbf{U}$  and  $\mathbf{\Sigma}$  will be computed for the receiver to perform symbol detection. Also, the angles representing  $\mathbf{V}$  will be computed such that they can be sent back to the transmitter. To compute angles, it is natural to use Givens rotation in our algorithms and to use CORDIC module [15, 16] in our hardware architectures for the precoding sub-system.

#### 3.1. Algorithm for the SVD of $\mathbf{H}$

In the conventional algorithms [7] for performing SVD, the first step is to bi-diagonalize the  $\mathbf{H}$ . Because  $\mathbf{H}$  is of size  $4 \times 2$ , we can instead, in our first step, use complex Givens rotation [17] to QR-decompose the  $\mathbf{H}$ , i.e.,

$$\underbrace{\begin{bmatrix} h_{1,1} & h_{1,2} \\ h_{2,1} & h_{2,2} \\ h_{3,1} & h_{3,2} \\ h_{4,1} & h_{4,2} \end{bmatrix}}_{\mathbf{H}} = \underbrace{\begin{bmatrix} q_{1,1} & q_{1,2} \\ q_{2,1} & q_{2,2} \\ q_{3,1} & q_{3,2} \\ q_{4,1} & q_{4,2} \end{bmatrix}}_{\mathbf{Q}} \underbrace{\begin{bmatrix} r_{1,1} & r_{1,2} \\ 0 & r_{2,2} \end{bmatrix}}_{\mathbf{R}}. \quad (4)$$

The diagonal entries  $r_{1,1}$  and  $r_{2,2}$  are positive, but the entry  $r_{1,2}$  is complex-valued. The complex-valued Jacobi algorithm [12, 13] can then be applied to diagonalize the  $2 \times 2 \mathbf{R}$  by

$$\begin{bmatrix} \cos(\theta_\lambda) & -\sin(\theta_\lambda) \\ \sin(\theta_\lambda) & \cos(\theta_\lambda) \end{bmatrix} \begin{bmatrix} 1 & 0 \\ 0 & e^{j\theta_\phi} \end{bmatrix} \mathbf{R} \begin{bmatrix} 1 & 0 \\ 0 & e^{-j\theta_\phi} \end{bmatrix} \\ \times \begin{bmatrix} \cos(\theta_\rho) & -\sin(\theta_\rho) \\ \sin(\theta_\rho) & \cos(\theta_\rho) \end{bmatrix} = \begin{bmatrix} \sigma_1 & 0 \\ 0 & \sigma_2 \end{bmatrix}, \quad (5)$$

where  $\theta_\phi = \tan^{-1}(\Im\{r_{1,2}\}/\Re\{r_{1,2}\})$  is the angle of  $r_{1,2}$ . Also, the  $\theta_\lambda$  and  $\theta_\rho$  can be easily obtained from the relationships

$$\begin{cases} \theta_\lambda + \theta_\rho = \tan^{-1}\left(\frac{|r_{1,2}|}{r_{2,2} - r_{1,1}}\right) \\ \theta_\lambda - \theta_\rho = \tan^{-1}\left(\frac{|r_{1,2}|}{r_{2,2} + r_{1,1}}\right) \end{cases}. \quad (6)$$

The singular values can be expressed as

$$\sigma_1 = \frac{\sqrt{|r_{1,2}|^2 + (r_{2,2} + r_{1,1})^2} + \sqrt{|r_{1,2}|^2 + (r_{2,2} - r_{1,1})^2}}{2} \quad (7)$$

and

$$\sigma_2 = \frac{\sqrt{|r_{1,2}|^2 + (r_{2,2} + r_{1,1})^2} - \sqrt{|r_{1,2}|^2 + (r_{2,2} - r_{1,1})^2}}{2}. \quad (8)$$

Substituting (5) into (4), we obtain the SVD of  $\mathbf{H}$  as

$$\underbrace{\begin{bmatrix} \cos(\theta_\lambda) & -\sin(\theta_\lambda) \\ \sin(\theta_\lambda) & \cos(\theta_\lambda) \end{bmatrix}}_{\mathbf{U}^H} \begin{bmatrix} 1 & 0 \\ 0 & e^{j\theta_\phi} \end{bmatrix} \mathbf{Q}^H \mathbf{H} \\ \times \underbrace{\begin{bmatrix} 1 & 0 \\ 0 & e^{-j\theta_\phi} \end{bmatrix}}_{\mathbf{V}} \underbrace{\begin{bmatrix} \cos(\theta_\rho) & -\sin(\theta_\rho) \\ \sin(\theta_\rho) & \cos(\theta_\rho) \end{bmatrix}}_{\mathbf{\Sigma}} = \begin{bmatrix} \sigma_1 & 0 \\ 0 & \sigma_2 \end{bmatrix}. \quad (9)$$

The value of  $\mathbf{U}^H$  and  $\mathbf{V}$  are expressed in terms of matrix  $\mathbf{Q}^H$  and angles  $\theta_\phi, \theta_\lambda$ , and  $\theta_\rho$ . For clarity, the detailed steps to perform the

SVD of  $\mathbf{H}$  are illustrated in Fig. 2. Note that the computed angles  $\theta_\rho$  and  $\theta_\phi$  are to be sent back to the transmitter such that the value of precoding matrix  $\mathbf{V}$  can be constructed according to (9). The value of  $\mathbf{U}^H$  are constructed according to (9) using the value of  $\mathbf{Q}^H$ , and, angles  $\theta_\lambda$  and  $\theta_\phi$ . The values of  $\mathbf{U}$  and  $\mathbf{\Sigma}$  will be used by the receiver to detect precoded signals.

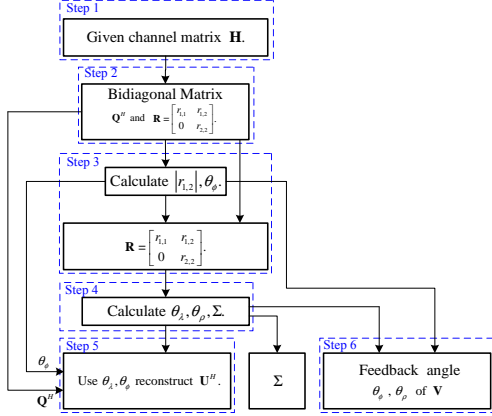


Fig. 2. The detailed steps of our algorithm to compute the SVD of  $\mathbf{H}$ .

### 3.2. Hardware Architecture for the SVD of $\mathbf{H}$

Based on the algorithm in Fig. 2, we propose the VLSI architecture for the precoding sub-system in Fig. 3. The bi-diagonalization and SVD blocks are associated with the computations revealed by (4) and (9), respectively.

Since the algorithm is expressed in terms of angles, the CORDIC modules are used in our architecture. Among the various types of CORDIC modules [15], the conventional CORDIC module to compute an angle or to rotate by an angle  $\omega$  is used. The two angles,  $\omega_a$  and  $\omega_b$ , computed by two different conventional CORDIC modules can be added or subtracted to produce an angle,  $\omega_a + \omega_b$  or  $\omega_a - \omega_b$ , that is to be used by another conventional CORDIC module. Each CORDIC module contains a pre-rotation, 9 shift-and-add iterations (micro-rotations), and a constant multiplication by 0.6073. The word length of each real number is determined to be 16 bits. Each of the CORDIC modules that is denoted by “VM/RM” computes the angle in the vectoring mode and then performs angle rotation in the rotation mode. Each CORDIC module that is denoted by “RM” performs angle rotation only using the angle information provided by another CORDIC module. As in [16], three pipeline registers are inserted in each CORDIC module to shorten the critical path of the designed circuit.

Illustrated in Fig. 4, the bi-diagonalization block performs the QRD in (4). Because only QRD of a  $4 \times 2$  matrix is to be computed, the bi-diagonalization block is obtained by removing some of processing elements of the triangular systolic array in [17, Fig. 1]. Each of the complex Givens rotation (CGR) and reduced CGR modules is comprised of CORDIC modules illustrated in Fig. 5. A total of 17 CORDIC modules are included in the bi-diagonalization block. When channel matrix  $\mathbf{H}$  is input to the bi-diagonalization module, all the CGR and reduced CGR modules perform the CORDIC vectoring operation to compute the angles for triangulating matrix  $\mathbf{R}$ . When a following identity matrix is input to the bi-diagonalization

block, all the CORDIC modules perform CORDIC rotation to compute the value of  $\mathbf{Q}^H$ . The delay units (DUs) are inserted to maintain timing synchronization of the signals.

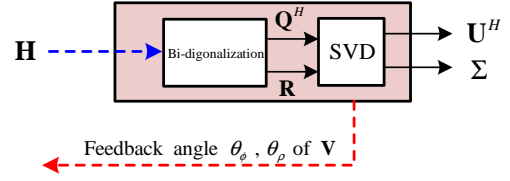


Fig. 3. The hardware architecture of our precoding sub-system.

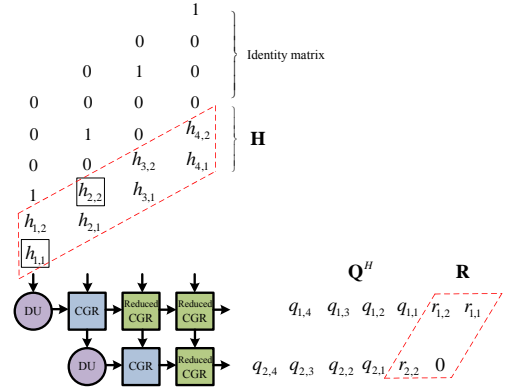


Fig. 4. The bi-diagonalization block in Figure 3.

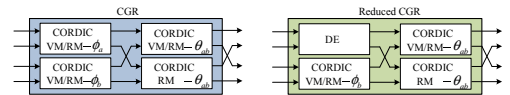


Fig. 5. The CGR and reduced CGR sub-modules in Figure 4.

The SVD block in Fig. 3 is expanded in Fig. 6. The demultiplexer selects either the  $\mathbf{R}$  or  $\mathbf{Q}$  to be passed to the following circuits. When  $\mathbf{R}$  is passed, the CORDIC modules that are denoted by “VM” perform CORDIC vectoring operations to compute the three angles  $\theta_\phi$ ,  $\theta_\lambda + \theta_\rho$ , and  $\theta_\lambda - \theta_\rho$ . The two angles,  $\theta_\lambda + \theta_\rho$  and  $\theta_\lambda - \theta_\rho$ , are summed/subtracted to produce angles  $\theta_\lambda$  and  $\theta_\rho$ . As revealed by (6), the CORDIC modules that are associated with angles  $\theta_\lambda - \theta_\rho$  and  $\theta_\lambda + \theta_\rho$  produce amplitudes  $\sqrt{|r_{1,2}|^2 + (r_{2,2} - r_{1,1})^2}$  and  $\sqrt{|r_{1,2}|^2 - (r_{2,2} - r_{1,1})^2}$ , respectively, in their vectoring operations. Thus, due to the results in (7) and (8), simple addition and subtraction are applied to the outputs of the two CORDIC modules to produce singular values  $\sigma_1$  and  $\sigma_2$ . On the other hand, when  $\mathbf{Q}^H$  is passed, the CORDIC modules that are denoted by “RM” apply CORDIC rotations to  $\mathbf{Q}^H$  to obtain  $\mathbf{U}^H$ .

### 3.3. Implementation Results

The architecture in Fig. 3 was described in Verilog HDL and synthesized by the Synopsys Design Compiler, the result of which is compared with several architectures in Table 1. The throughput rate

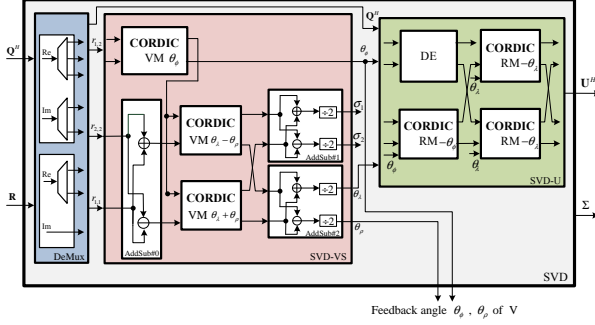


Fig. 6. The SVD block in Figure 3.

is computed according to

$$\begin{aligned} & \text{Normalized SVD Throughput Rate (matrices/sec)} \\ &= \frac{\text{Operating Frequency}}{\text{Processing Cycles}} \times \frac{\text{Technology}}{90 \text{ nm}}. \end{aligned} \quad (10)$$

Because of the pipeline structure in the architecture, a new matrix and an identity matrix can be input to the architecture every 6 clock cycles, which is the processing cycles in (10). It only takes 3.33 and 6.79  $\mu\text{s}$  for our architecture to compute the SVD of channel matrices for the 56 and 114 channel matrices, respectively, at all data sub-carriers of the IEEE 802.11n/ac signal.

Table 1. Comparisons of hardware architectures.

Architecture	[7]	[8]	[10]	This work
Algorithm	GK-SVD	SL-SVD	Adaptive SVD	QRD + Jacobi
Matrix size	$4 \times 4$	$4 \times 4$	$4 \times 4$	$4 \times 2$
Computed values	$\Sigma, \mathbf{V}$	$\mathbf{U}, \Sigma, \mathbf{V}$	$\mathbf{U}, \Sigma, \mathbf{V}$	$\mathbf{U}, \Sigma,$ angles of $\mathbf{V}$
Technology	180 nm	90 nm	90 nm	90 nm
Gate count	42.3K	120K	543.9K	122.8K
Frequency	149 MHz	182MHz	101.2 MHz	100.7 MHz
SVD throughput (matrices / sec.)	303K	7M	479.1K	16.8M

#### 4. PRECODING SUB-SYSTEM FOR THE DOWNLINK TRANSMISSION

The precoded sub-system for the downlink transmission with  $N_r = N_s = 2$  and  $N_t = 4$  is studied. Since the transmission for the WLAN is time-division duplex (TDD) [18], the channel matrix  $\mathbf{H}^T$  for this scenario is of size  $2 \times 4$ . Using the results in (9), we write the SVD of  $\mathbf{H}^T$  as

$$\underbrace{\begin{bmatrix} \cos(\theta_\rho) & \sin(\theta_\rho) \\ -\sin(\theta_\rho) & \cos(\theta_\rho) \end{bmatrix}}_{\mathbf{V}^T} \begin{bmatrix} 1 & 0 \\ 0 & e^{-j\theta_\phi} \end{bmatrix} \mathbf{H}^T \\ \times \mathbf{Q}^* \underbrace{\begin{bmatrix} 1 & 0 \\ 0 & e^{j\theta_\phi} \end{bmatrix}}_{\mathbf{U}^*} \underbrace{\begin{bmatrix} \cos(\theta_\lambda) & \sin(\theta_\lambda) \\ -\sin(\theta_\lambda) & \cos(\theta_\lambda) \end{bmatrix}}_{\Sigma} = \begin{bmatrix} \sigma_1 & 0 \\ 0 & \sigma_2 \end{bmatrix}. \quad (11)$$

For this channel matrix  $\mathbf{H}^T$ , the precoding sub-system can still feedback the angles representing  $\mathbf{U}$  to the transmitter and generates the values of  $\Sigma$  and  $\mathbf{V}$  to be used by the receiver for detecting precoded symbols. Thus, the SVD algorithm here is similar to that in Subsection 3.1.

By slightly modifying the architecture introduced in Subsection 3.2, we can obtain the architecture for the precoding sub-system for the downlink. The proposed architecture is comprised of two blocks as in Fig. 3. Because only the angles representing  $\mathbf{U}$  are to be computed, the CORDIC modules in the bi-diagonalization block in Fig. 4 perform CORDIC vectoring operations only. Thus, the CORDIC modules that perform CORDIC rotations only in the sub-modules of Fig. 5 can be eliminated. A total of 12 CORDIC modules is required in the bi-diagonalization block. The SVD block here is even simpler than the one in Fig. 6, which is equal to 6. Angles  $\theta_\phi, \theta_\lambda$ , and those 12 angles produced by the bi-diagonalization block are to be feedback to the transmitter side. Also, only the input  $\mathbf{H}$  is required; the following identity matrix in Fig. 4 is not required to be input. New channel matrices can be input to the architecture every 2 clock cycles.

The architecture for this scenario is described and synthesized. The required gate count is 94K gates. The SVD throughput rate that this architecture can provide is 50.4M matrices per second when operating at clock frequency 100.7 MHz. It only takes 1.11 and 2.26  $\mu\text{s}$  for our architecture to compute the SVD of channel matrices for the 56 and 114 channel matrices, respectively, at all data sub-carriers of the IEEE 802.11n/ac signal.

#### 5. CONCLUSION

Our architectures of the precoding sub-systems are the first architectures to deliver the compressed beamforming weights feedback for both the uplink and downlink transmissions in the IEEE 802.11n/ac WLAN. Utilizing the systolic array and non-iterative Jacobi algorithm, our architectures can compute the feedback information rapidly and therefore suitable for the practical system.

#### 6. ACKNOWLEDGMENT

The authors greatly appreciate the National Chip Implementation Center of Taiwan for providing technical support over the duration of this work.

#### 7. REFERENCES

- [1] D. Love, R. Heath Jr., V. Lau, D. Gesbert, and B. Rao, "An overview of limited feedback in wireless communications systems", *IEEE J. Selected Areas Commun.*, vol. 26, no. 8, pp. 1341-1365, Aug. 2008.
- [2] E. Perahia and R. Stacey, *Next Generation Wireless LANs 802.11n and 802.11ac*. 2nd Ed., Cambridge University Press, 2013.
- [3] J. Lee, J.-K. Han, and J. Zhang, "MIMO technologies in 3GPP LTE and LTE-Advanced," *EURASIP Journal Wireless Commun. Networking*, 2009.

- [4] Y.-H. Lin, Y.-H. Chen, C.-Y. Chu, C.-Z. Zhan, and A.-Y. Wu, "Dual-mode low-complexity codebook searching algorithm and architecture for LTE/LTE-advanced systems," *IEEE Trans. Signal Proc.*, vol. 61, no. 14, pp. 3545-3562, July 2013.
- [5] T.-H. Liu, C.-N. Chiu, and C.-Y. Lin, "Fast codeword selection for limited feedback beamforming MIMO systems using breadth-first tree search," *IET-Commun.*, vol. 7, no. 6, pp. 531-537, June 2013.
- [6] E. Dahlman, S. Parkvall, and J. Skold, *4G LTE/LTE-Advanced for Mobile Broadband*. Academic Press, 2011.
- [7] C. Senning, C. Studer, P. Luethi, and W. Fichtner, "Hardware-efficient steering matrix computation architecture for MIMO communication systems," In Proc. *IEEE Int. Symp. Circuits and Systems (ISCAS)*, pp. 304-307, 2008.
- [8] C. Z. Zhan, Y. L. Chen, and A. Y. Wu, "Iterative superlinear-convergence SVD beamforming algorithm and VLSI architecture for MIMO-OFDM systems," *IEEE Trans. Signal Processing*, vol. 60, no. 6, pp. 3264-3277, June 2012.
- [9] D. Markovic, B. Nikolic, and R. W. Brodersen, "Power and area minimization for multidimensional signal processing," *IEEE Journal Solid-State Circuits*, vol. 42, no. 4, pp. 922-934, Apr. 2007.
- [10] Y. L. Chen, C. Z. Zhan, T. J. Jheng, and A. Y. Wu, "Reconfigurable adaptive singular value decomposition engine design for high-throughput MIMO-OFDM systems," *IEEE Trans. Very Large Scale Integration (VLSI) Systems*, vol. 21, no. 4, pp. 747-760, 2013.
- [11] Y.-T. Hwang, W.-D. Chen, and C.-R. Hong, "A low complexity geometric mean decomposition computing scheme and its high throughput VLSI implementation," *IEEE Trans. Circuits and Systems I: Regular Papers*, vol. 61, no. 4, pp. 1170-1182, Apr. 2014.
- [12] J. R. Cavallaro and A. C. Elster, "A CORDIC processor array for the SVD of a complex matrix," In *SVD and Signal Processing II: Algorithms, Analysis and Applications*, pp. 227-239, 1991.
- [13] N. D. Hemkumar and J. R. Cavallaro, "A systolic VLSI architecture for complex SVD," In Proc. *1992 IEEE Int. Symp. Circuits and Systems*, May 1992, pp. 1061-1064.
- [14] D. Love, and R. Heath Jr., "Equal gain transmission in multiple-input multiple output wireless systems", *IEEE Trans. Commun.*, vol. 31, no. 7, pp. 1102-1110, July 2003.
- [15] P. Meher, J. Valls, T.-B. Juang, K. Sridharan, and K. Maharatna, "50 Years of CORDIC: algorithms, architectures, and applications," *IEEE Trans. Circuits and Systems I: Regular Papers*, vol. 56, no. 9, pp. 1893-1907, Sept. 2009.
- [16] Z. Y. Huang and P. Y. Tsai, "Efficient implementation of QR decomposition for gigabit MIMO-OFDM systems," *IEEE Trans. Circuits and Systems I: Regular Papers*, vol. 58, no. 10, pp. 2531-2542, Oct. 2011.
- [17] A. Maltsev, V. Pestretsov, R. Maslennikov, and A. Khoryaev, "Triangular systolic array with reduced latency for QR decomposition of complex matrices," In Proc. *IEEE Int. Symp. Circuits and Systems (ISCAS)*, May 2006, pp. 385-388.
- [18] G. Lebrun, T. Ying, and F. Faulner, "MIMO transmission over a time-varying TDD channel using SVD," *IEEE Trans. Wireless Commun.*, vol. 4, no. 2, pp. 757-764, Mar. 2005.